A Network Model for the Kinetics of Bioclogged Flow Diversion for Enhanced Oil Recovery

Lopez Pena, Luis; Meulenbroek, Bernard; Vermolen, Fred

DOI
10.3997/2214-4609.201601769

Publication date
2016

EAGE

ECMOR XV

Mo P014

A Network Model for the Kinetics of Bioclogged Flow Diversion for Enhanced Oil Recovery

L.A. López Peña* (TU Delft), B. Meulenbroek (TU Delft) & F.J. Vermolen (TU Delft)

SUMMARY

After the primary extraction in oil reservoirs up to 60 % of the oil remains trapped in the reservoir (Sen, 2008). Therefore, different mechanisms have been developed to get the oil out to the reservoir. One of these techniques is Microbial Enhanced Oil Recovery (MEOR) which is a technique used to produce more oil in a secondary extraction by using microbes in the reservoir. The main effects caused by microbes in oil recovery is the reduction of the interfacial tension between oil and water, wettability change of the rock and bioclogging caused by the growth and development of biofilm. Among these mechanisms, interfacial tension reduction and biclogging is thought to have the greatest impact on recovery (Sen, 2008). In this work, we describe the growth of biofilm, the growth of the microbial population and the transport of nutrients using a pore network model. We follow the previous models of Thullner et al. (Thullner, 2008) and Ezeuko et al. (Ezeuko, 2011) in which the biofilm is considered as a permeable layer. We consider the biofilm and the bacteria separately. Additionally, we assume that once a tube is full with biofilm, this biofilm can spread to the neighboring tubes. Finally, we study the changes in the hydrodynamic properties of the medium caused by the plugging of the pores and we study the flow diversion of water caused by plugging of the high permeability zones.

Introduction

Microbial Enhanced Oil Recovery (MEOR) is a technique in which the growth of bacteria and the resulting by-products are used in order to increase residual oil production in a tertiary oil recovery method. MEOR techniques involve the use of indigenous microorganisms or the injection of selected external bacteria into the reservoir to produce the desired by-products. Typically, in MEOR techniques, bacterial population growth is supported by the injection of nutrients into the reservoir [18].

Microbes enhance oil displacement by different processes: interfacial tension reduction, rock wettability change and increment of the waterflood sweep efficiency caused by selective plugging [1]. Among these mechanisms, interfacial tension reduction and selective plugging are thought to have the greatest impact on recovery [18]. During selective plugging, bacteria grow and adhere, within a self produced matrix of extra cellular polymeric substances (EPS), to the walls of the pores of high permeability zones. The bacteria adhered and the self produced matrix is referred as biofilm. Biofilm growth leads to the plugging of the pores in high permeability zones, causing the diversion of the water-flood from the thief zones towards oil-rich areas.

The applicability of MEOR techniques to increase oil extraction has been shown in laboratory experiments [3, 25, 11] and field trials [11]. In laboratory experiments, it has been shown that biofilm accumulates in high permeability zones, diverting the water-flood towards oil trapped zones [14]. Field trials have been implemented in order to verify the effectiveness of microbial processes predicted in laboratories. The Alton field in Australia showed that the net oil production increased 40% and it continued after 12 months of treatment [19]. A field study in Canada showed that selective plugging is one of the most promising processes in MEOR techniques [8]. The extent of success in oil recovery using MEOR techniques depends on several factors such as individual reservoir characteristics: lithology, porosity, permeability, temperature and oil composition. Additionally, microbial activity, bacterial composition and concentration of nutrients determine the performance of MEOR. Therefore, the prediction of the failure or success of the MEOR techniques is limited by the lack of measures in microbial activity [18]. However, it is possible to describe quantitatively the relationships between reservoir characteristics, microbes and operating conditions [4].

The development of mathematical and numerical models predicting the bacterial population growth, nutrients transport and in situ production of by-products is of vital importance to develop a proper field strategy [18]. Several numerical models have been developed to describe biofilm growth. There exist continuum Darcy models [23], bacterially-based models [12], Lattice-Boltzmann-based simulations [13, 17] and Pore Network Models (PNM) [6, 22, 20, 5, 7]. Frequently, in biofilm growth models, the porous media consists of three components: the grains, the biofilm which grows on the walls of the solid grains and the liquid in the pore space. The grains are assumed to be impermeable to the liquid and the nutrients, therefore, hydrodynamic model equations are written only for the liquid and biofilm [13]. In the flow regimes that we are considering now, we also assume that the grains are non-deformable.

In PNMs, pores are considered as cylindrically interconnected tubes in which the water can flow. The dynamics of the problem is described by transport of nutrients through the network, bacterial population growth and biofilm development. Transport of nutrients is carried out within an aqueous phase and is described by a convection diffusion equation with a reaction term that considers the consumption of nutrients caused by bacterial population growth. The bacterial population will determine the development of biofilm in the pores of the medium. This biofilm will grow and will change the radii of the pores, leading to a modification in the dynamics of the fluid that carries the nutrients through the network [6, 22, 20, 5]. The geometric properties of the network such as connectivity, coordination number or coordination number distribution have an influence on transport of solute and in multiphase flow in porous systems [15].

Among PNMs different approaches have been used to study the evolution of the fluid dynamics of the system and the biofilm growth in the network. Commonly, the biofilm is treated as an impermeable layer [22, 20, 9]. However, the assumption that nutrients can flow through the biofilm produces a better match

with laboratory experiments [21]. Thullner et al. [21] considered that the flow in each of the tubes is described by a modified form of the Poiseuille flow where the flux through the biofilm and through the void space is taken into account. Considering that nutrients can also flow through the biofilm phase, Ezeuko et al. [6] used two different diffusion coefficients, one for diffusion through the water-water interface and another for the water-biofilm interface.

The Monod kinetics equation is usually used to describe the growth of bacteria in the pores [6, 21, 20, 5], this equation relates the growth rate of bacteria with the concentration of nutrients available in the network.

Even though the biofilm phase and the bacteria phase are two different phases, the distinction in PNM's between biofilm and bacteria has not been made explicit in the literature. In Thullner et al. [21] no distinction between biofilm and bacteria is taken into account while Ezeuko et al. [6] consider the biofilm as an attached phase of bacteria.

In this work, we model the growth of biofilm, the growth of the bacteria population and the transport of nutrients in a porous medium. As in the previous works of Thullner et al. [21] and Ezeuko et al. [6], we consider the biofilm phase as a permeable layer which means nutrients can travel through the biofilm phase due to advection. However, diffusion was considered only in the water phase. Note that we consider the bacteria and the biofilm separately. Additionally, we consider that the excess volume of biofilm can be spread to the neighboring tubes. Finally, we study the possibility of flow diversion from thief zones to areas of low permeability by means of bioclogging. We model two regions with different permeabilities and we compute the flow out of the low permeability region, since this flow mimics the amount of oil that can be produced from the low permeability zone.

This paper consists of four sections. In Section 2, in the Mathematical model subsection, we describe the physical, mathematical and biological considerations that are involved in the process of bioclogging in a porous medium. We illustrate how we model the porous medium, the injection of nutrients, the growth of bacteria, and the growth and development of biofilm. In Section 2, in the Numerical method subsection, the numerical method used is described and the computational steps are explained. In Section 3, the results and discussion are presented. Finally, in Section 4 the conclusions are drawn and the outlook to other problems are presented.

Method and Theory

Mathematical Model

We represent the porous medium as a 2D network composed of interconnected cylindrical tubes. The point where these tubes are connected is called a node of the network and is indexed as node n_i. The tube between the node n_i and n_j is indexed as the tube t_{ij}. A Rayleigh distribution for the radii was used. In addition, it is assumed that all the tubes have the same length l. The number of tubes connected in each node is four for interior nodes, three for boundary nodes and two for the nodes in the corner of the network (see Figure 1). In Figure 2 the ordering of the nodes is presented.

We assume that bacteria is necessary for the biofilm growth, therefore, we consider that 4% of the tubes have an initial concentration of bacteria b_0. Initially, nutrients are not present in the network, hence, nutrients need to be injected through the network and transported within a fluid.

In this work, we consider the biofilm as a permeable layer in which nutrients are able to be transported as well. Additionally, we consider a single concentration in each tube, hence, no distinction between the concentration in the biofilm phase and the concentration in the water phase was made.

We define the thickness of the biofilm in the tube t_{ij} as $r_{b_{ij}}$, the radius of tube available for water by $r_{w_{ij}}$ and the total radius of the tube by R_{ij} (see Figure 1).

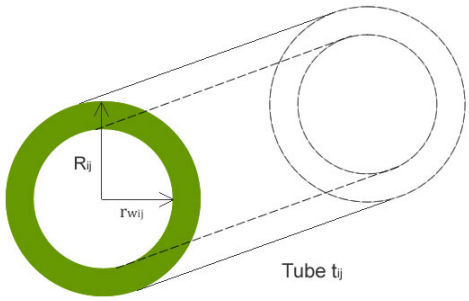

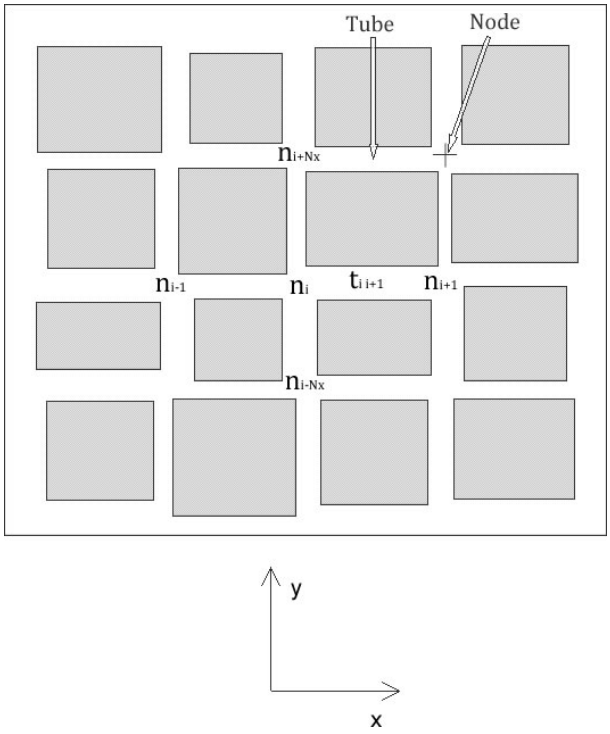

Figure 1 *Pore Network and tubes.*

$$
\begin{array}{ccccc}
.. & .. & .. & .. & n_{N_x * N_y} \\
.. & .. & .. & .. & .. \\
.. & .. & n_{i+N_x} & .. & .. \\
.. & n_{i-1} & n_i & n_{i+1} & .. \\
.. & .. & n_{i-N_x} & .. & .. \\
n_{Nx+1} & .. & .. & .. & .. \\
n_1 & n_2 & .. & .. & n_{Nx}
\end{array}
$$

Figure 2 *Order of the nodes in the network.*

The volumetric flow of the aqueous phase q_{ij} in the tube t_{ij} is described by a modified form of the Poiseuille equation [21],

$$q_{ij} = \frac{\pi}{8\mu l}[r_{w_{ij}}^4 + (R_{ij}^4 - r_{w_{ij}}^4)\beta^{-1}]\Delta p, \tag{1}$$

where Δp is the pressure drop between the neighboring nodes n_i and n_j, μ is the viscosity of water that flows in the bulk, β is the ratio between the viscosity of water flowing through the biofilm and the viscosity of water flowing through the bulk and l is the length of the tube. According to Thullner et al. [21] $\beta = 10^3$ is a good approximation for a permeable biofilm.

Mass conservation is imposed in each of the nodes. For the node n_i we have

$$\sum_{j \in S_i} q_{ij} = 0, \tag{2}$$

where $S_i = \{j \mid n_j \text{ is adjacent to the node } n_i\}$ and further q_{ij} is the flux in the tubes connected to node n_i.

The transport of nutrients is described by an advection diffusion reaction equation. We denote the concentration of nutrients as C $[kg/m^3]$,

$$\frac{\partial C}{\partial t} = -\mathbf{u} \cdot \nabla C + D\nabla^2 C - \frac{\lambda_b^+}{Y}\frac{C}{E_{bs} + C}b, \tag{3}$$

where b is the biomass concentration, λ_b^+ is a microbial specific consumption rate, Y is the yield coefficient, E_{bs} is a saturation constant, D is the diffusion coefficient and $\mathbf{u}$ is the velocity which is related to the flux $\mathbf{q}$ by $\mathbf{u} = \mathbf{q}/A$, where A is the area of the cross section of the tube.

The growth of the biomass concentration b $[kg/m^3]$ is given by

$$\frac{\partial b}{\partial t} = \frac{\lambda_b^+}{Y}\frac{C}{E_{bs} + C}b, \tag{4}$$

in which the growth rate is given by Monod Kinetics. In this equation λ_b^+ is a microbial specific growth rate, Y is the yield coefficient and E_{bs} is a saturation constant. We consider the biofilm as an adsorbed phase on the walls of the tubes. We describe the growth and development of the biofilm by its concentration Φ expressed as mass per pore volume unit.

The evolution of the concentration Φ is described by,

$$\frac{\partial \Phi}{\partial t} = \begin{cases} \lambda_\Phi^+ \dfrac{C}{E_{\Phi_s} + C}\Phi - \lambda_\Phi^- \Phi, \text{ if } V_{bf} < V & \text{(5a)} \\ 0, \text{ if } V_{bf} \geq V & \text{(5b)} \end{cases}$$

in this equation λ_Φ^+ is a microbial specific growth rate, $E_{\Phi s}$ is a saturation constant and λ_Φ^- is a decay rate for the biofilm due to shear stress, V_{bf} is the volume of biofilm and V is the total pore volume. If

the volume of the biofilm is equal or larger than the volume of the tube, we consider that the biofilm can not grow anymore. The concentration of biofilm can be converted into volume of biofilm, assuming constant density of the biofilm and constant pore volume in each tube.

The volume of the biofilm $V_{bf_{ij}}$ in the tube t_{ij} is determined by

$$V_{bf_{ij}} = \frac{\Phi_{ij}}{\rho_{bf}} V_{ij}, \tag{6}$$

where Φ_{ij} is the concentration of biofilm, V the total pore volume and ρ_{bf} is the density of the biofilm.

In this model we take into account that biofilm can spread to the neighboring tubes when an excess volume of biofilm is produced. For example, if for the tube t_{ij} we have that $V^t_{bf_{ij}} < V_{ij}$ equation (5a) is used to compute the biofilm concentration Φ^{t+1}_{ij} at the next time step. The volume of biofilm at time $t+1$ for the tube t_{ij} can be computed using equation (6), if $V^{t+1}_{bf_{ij}} > V_{ij}$ and excess volume of biofilm is produced in the tube t_{ij},

$$V_{ex_{ij}} = V_{bf_{ij}} - V_{ij}. \tag{7}$$

This excess volume of biofilm is distributed to the neighboring tubes according to the spreading potential, defined for each neighboring tube t_{ij_k} as [6],

$$w_{ij_k} = \frac{q_{ij_k} C_{ij_k}}{\rho_{bf} V_{ij_k}}, \tag{8}$$

where q_{ij_k} is the volumetric flow, C_{ij_k} is the concentration of nutrients, V_{ij_k} is the total pore volume in the neighboring tube t_{ij_k} and ρ_{bf} is the density of the biofilm. The biofilm is spread only to the downstream tubes. The volume excess given to the tube t_{ij_k} is defined as,

$$V_{ex_{ij_k}} = \frac{V_{ex_{ij}} w_{ij_k}}{\sum_{j_k} w_{ij_k}}, \tag{9}$$

the sum is over all the neighboring downstream tubes.

The total concentration of biofilm $\Phi^{tot}_{ij_k}$ in the neighboring tube that received the excess volume will be adjusted according to,

$$\Phi^{tot}_{ij_k} = \Phi_{ij_k} + \rho_{bf} \frac{V_{ex_{ij_k}}}{V_{ij_k}}. \tag{10}$$

in which the first term in the right hand side is the concentration computed using equation (5a) and the second term is the concentration due to the spreading of the biofilm. The total volume of biofilm $V^{tot}_{bf_{ij_k}}$ in the neighboring tubes is computed as,

$$V^{tot}_{bf_{ij_k}} = \frac{\Phi^{tot}_{ij_k}}{\rho_{bf}} V_{ij_k}. \tag{11}$$

Additionally, the concentration of the tube t_{ij} where the excess volume is produced is adjusted such that $V_{bf_{ij}} = V_{ij}$, therefore for the next time step equation (5b) holds and no more biofilm grows in the tube t_{ij}. Following equation (5a) and (5b) spreading of the biofilm from the tube t_{ij} to the neighboring tubes happens only once per tube.

The thickness of the biofilm can be computed from equation (11) and is coupled back to equation (1) and (2).

Numerical Method

In this section, we will outline the numerical procedure used in the model and the computational steps followed in this paper.

Substitution of equation (1) into (2) for each node n_i leads to a linear system for the pressure at the nodes, p_i, as unknowns. This system is solved assuming Dirichlet boundary conditions for the left and right boundary of the network and considering that there is no flow through the upper and lower boundary.

After solving the nodal pressures p_i, we can substitute their values into equation (1) to obtain the flux in each tube of the network.

The solution to equation (3) is approximated by the use of the finite differences scheme. Then, for each node, n_i, the advection diffusion reaction equation can be written as,

$$\frac{\Delta C_i}{\Delta t} = \left[\frac{\Delta C_i}{\Delta t}\right]_{adv} + \left[\frac{\Delta C_i}{\Delta t}\right]_{diff} + \left[\frac{\Delta C_i}{\Delta t}\right]_{reaction}. \tag{12}$$

The advection part can be written as,

$$\left[\frac{\Delta C_i}{\Delta t}\right]_{adv} = \left[\frac{{C_i}^{t+1} - {C_i}^{t}}{\Delta t}\right]_{adv} = \sum_{j\in\Omega_i} \frac{{q_{ij}}^{t}}{V_{ij}} ({C_j}^{t+1} - {C_i}^{t+1}), \tag{13}$$

where $\Omega_i = \{j \mid q_{ij}$ is directed towards the node n_i and n_j is a neighbor of n_i connected through the tube $t_{ij}\}$ and V_{ij} is the total volume of the tube.

The diffusion of nutrients through the water phase can be written as,

$$\left[\frac{\Delta C_i}{\Delta t}\right]_{diff} = \left[\frac{{C_i}^{t+1} - {C_i}^{t}}{\Delta t}\right]_{diff} = \frac{D_w}{l^2} \sum_{j\in S_i} ({C_i}^{t+1} - {C_j}^{t+1}) \frac{A^t_{w_{ij}}}{A_{tot_{ij}}}, \tag{14}$$

where D_w is the diffusion coefficient of the water in the free space available for the bulk water. Further, $A_{w_{ij}}$ is the area of the cross section of the bulk water in the tube t_{ij} and $A_{tot_{ij}}$ is the total area of cross section of the tube t_{ij}.

In this model, the reaction takes place in the tubes, therefore we describe the growth of bacteria b_{ij}, in the tube t_{ij}, as,

$$\frac{\Delta b_{ij}}{\Delta t} = \left[\frac{{b_{ij}}^{t+1} - {b_{ij}}^{t}}{\Delta t}\right] = \frac{\lambda_b^+}{Y} \left[\frac{{C_{ij}}^{t}}{E_{bs} + {C_{ij}}^{t}}\right] {b_{ij}}^{t+1}, \tag{15}$$

where $C_{ij} = \frac{C_i + C_j}{2}$ is the average concentration of the nodes n_i and n_j and represents the concentration in the tube t_{ij}.

However, in order to give an expression for the last term of equation (12) we need to know the concentration of bacteria in each node, b_i, then we average the concentration of bacteria of the tubes connected by the node n_i,

$$\frac{\sum_{j \in S_i} b_{ij} V_{ij}}{\sum_{j \in S_i} V_{ij}} = b_i, \tag{16}$$

Now the reaction term can be written as,

$$\left[\frac{\Delta C_i}{\Delta t}\right]_{reaction} = \left[\frac{C_i^{t+1} - C_i^t}{\Delta t}\right]_{reaction} = \frac{\lambda_b^+}{Y} \frac{C_i^{t+1}}{E_{B_s} + C_i^t} b_i^t. \tag{17}$$

The thickness of the biofilm is determined by the bacteria consumption as well as by the nutrients concentration. The change of biofilm concentration is given by

$$\frac{\Delta \Phi_{ij}}{\Delta t} = \left[\frac{{\Phi_{ij}}^{t+1} - {\Phi_{ij}}^t}{\Delta t}\right] = \lambda_\Phi^+ \left[\frac{{C_{ij}}^t}{E_{\Phi s} + {C_{ij}}^t}\right] \Phi_{ij}^{t+1} - \lambda_\Phi^- \Phi_{ij}^{t+1}. \tag{18}$$

The computational procedure used in this work is as follows. Firstly, the external pressure is imposed in the left and right boundary of the network. Subsequently, the pressure in each node is computed from the linear system resulting from the mass conservation in each node. For solving this system, we consider Dirichlet boundary conditions in the left and right boundaries and homogeneous Neumann boundary condition for the upper and lower boundary. The pressures in each node are used to compute the flux in each tube by means of equation (1). After this step, we proceed to solve the transport diffusion equation for the nutrients and we compute the concentration of nutrients in each node as well as the concentration of bacteria and the concentration of biofilm in the tubes. Subsequently, the volume of the biofilm is computed using equation (6). If an excess volume is produced in one of the tubes, the biofilm will spread to the neighboring tubes. The volume of biofilm will be computed taking into account the spreading volume. The thickness of the biofilm and the radius of the void space available for water is updated and this process starts again at the next time step (See Figure 3).

Results

First, we investigate the robustness of our results. The evolution of the concentration of nutrients through the network is studied without the presence of biofilm. We solve the advection diffusion equation for the concentration of nutrients with our model using a mesh with 200 x 10 elements and assuming that all the tubes in the network have the same radius. Under these conditions for the size of the mesh and the uniform size of the radii in all the tubes, we can compare the results with a model based on Continuous Random Walk Theory (CRWT) and with an analytic solution in one dimension [24]. The analytic solution of the advection diffusion equation (equation (3) without reaction term) in 1-D is given by:

$$c(x,t) = \frac{C_{in}}{2}\left[erfc\left(\frac{x - vt}{\sqrt{4Dt}}\right) + erfc\left(\frac{x + vt}{\sqrt{4Dt}}\right) exp\left(\frac{vx}{D}\right)\right] \tag{19}$$

in which erfc is the complementary error function, v the velocity and D the diffusion coefficient.

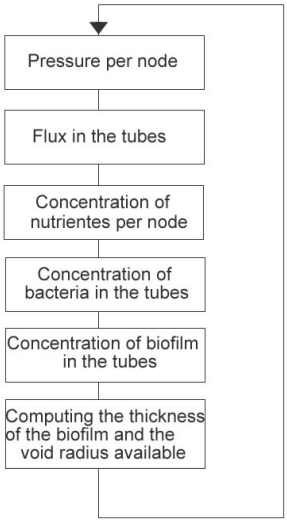

Figure 3 *Flow chart of the computational procedure for each time step.*

Figure 4 shows the results for the concentration of nutrients in one of the tubes closest to the outlet of the network for our model, a model based on continuous random walk theory (CRWT) and the analytic solution given by equation (19). We observe a good agreement between, the CTRW model, the analytic solution and our model.

The next step was to study the effects of the growth of biofilm on the dynamics of the system. For this second set of simulations, we used a mesh with 100 x 60 elements. A Rayleigh distribution for the radii of the tubes of the network was used. The mean radius is $r_{mean} = 12.2 \times 10^{-6}[m]$ (see Table 3).

Additionally, only 4% of the tubes were seeded with initial concentration of bacteria $b_0 = 1 \times 10^{-6}\ kg/m^3$ and initial concentration of biofilm $\phi_0 = 1 \times 10^{-6}\ kg/m^3$. The complete set of parameters for this second set of simulations is listed in Table 3.

Subsequently, we study the evolution of the flux over time. In Figure 5 the normalized flux is shown.

The normalized flux is defined as

$$Q_n = \frac{Q}{Q_0}, \tag{20}$$

where Q is the flux and Q_0 is the initial flux. We observe a decrease of the normalized flux due to the accumulation of biomass in the network. The injection of nutrients through the network and the bacterial conversion of them lead to the clogging of the pores and consequently to the reduction of the normalized flux of the network.

In Figure 6 we observe the average concentration of nutrients in the network, C_{av}. This concentration is defined as,

$$C_{av} = \frac{\sum_{ij} C_{ij} V_{ij}}{\sum_{ij} V_{ij}}, \tag{21}$$

in which C_{ij} is the concentration in the tube t_{ij} and V_{ij} is the total volume of the tube t_{ij}. The sums are over all the tubes in the network. We observe that the injection of nutrients is very fast, after approximately

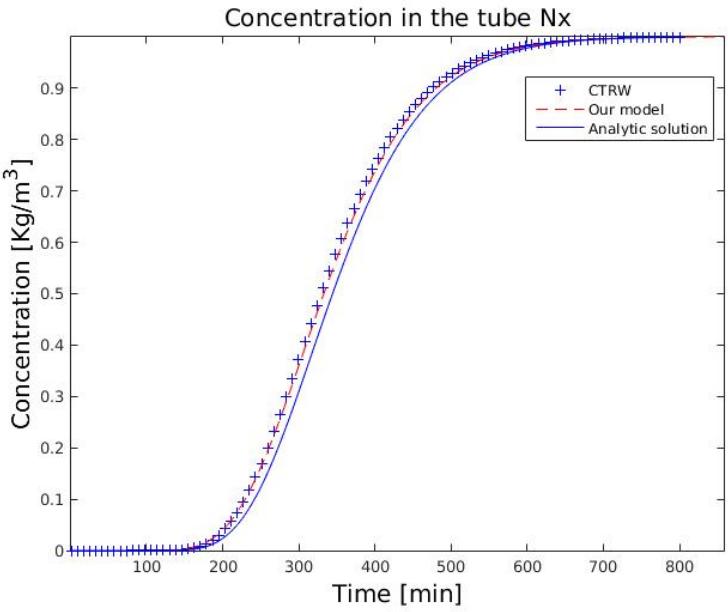

Figure 4 *Comparison of the solution of the advection diffusion equation of our model, CTRW and an analytic solution.*

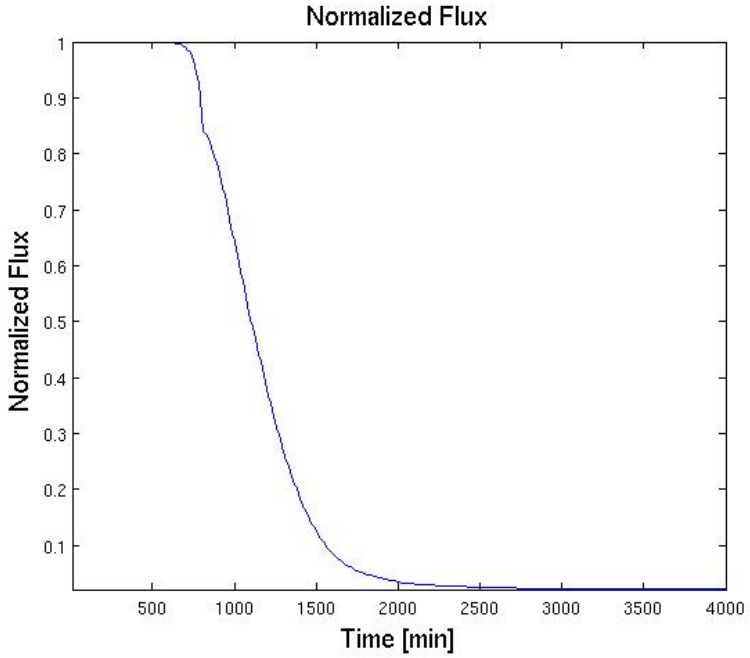

Figure 5 *Evolution of the normalized flux through the network.*

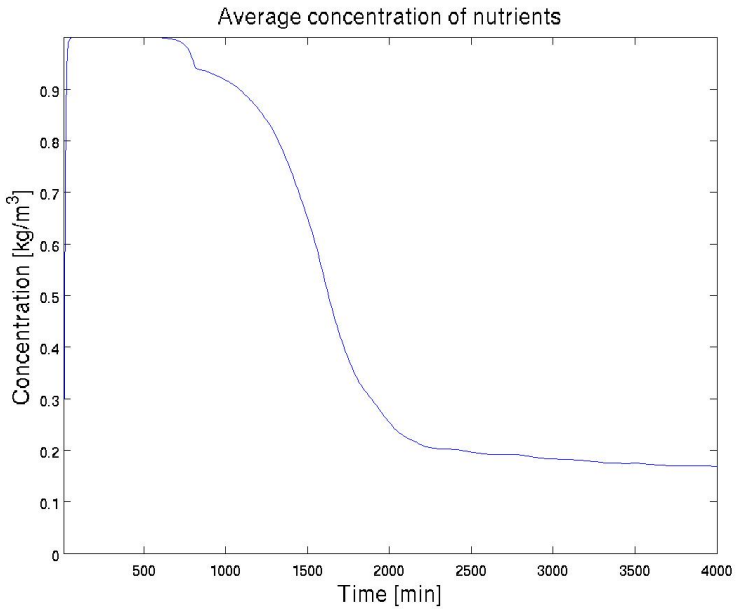

Figure 6 *Average concentration of nutrients in the network.*

50 minutes the nutrients are distributed over the whole network. The network is full of nutrients for approximately 700 min, hence, the biofilm grows uniformly across the network. After 600 minutes we observe a decrease in the average concentration of nutrients in the network due to the consumption by bacteria and biofilm.

Next, we examine the evolution in time of the volume of biofilm in the network. In Figure 7 the fraction of volume of biofilm is shown. The fraction of volume of biofilm, V_{pbf}, is defined as,

$$V_{pbf} = \frac{\sum_{ij} V_{bf_{ij}}}{\sum_{ij} V_{ij}}, \tag{22}$$

where $V_{bf_{ij}}$ is the volume of biofilm in tube t_{ij} and V_{ij} is the total pore volume of the tube t_{ij}. After 3000 minutes, we observe that approximately 70% of the void space of the network is occupied by the volume of biofilm. Since the biofilm growth in the network is distributed uniformly over the network, there is no preferential growth of the biofilm at the inlet of the network and hence, more biomass is necessary to reduce the flux through the network.

For this set of simulations we used 400 time steps, with the size of the time step $dt = 10\ [min]$.

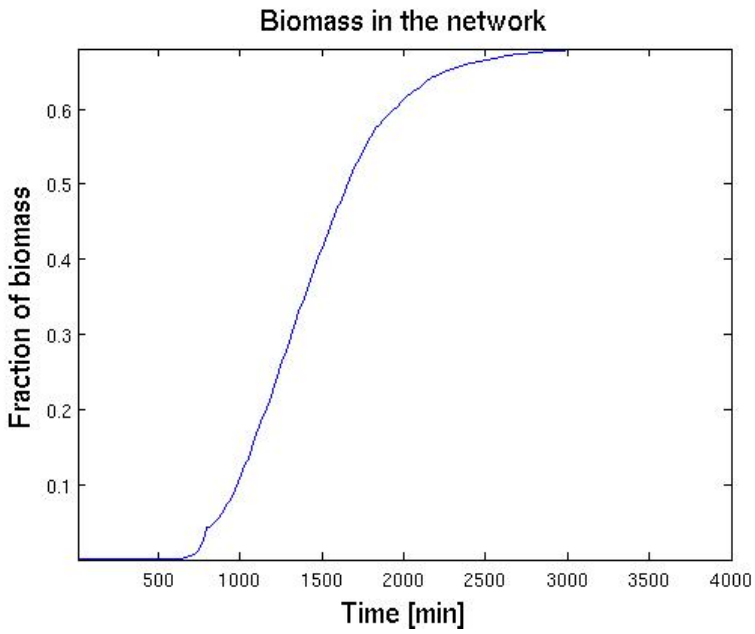

Figure 7 *Evolution of the biomass in the network.*

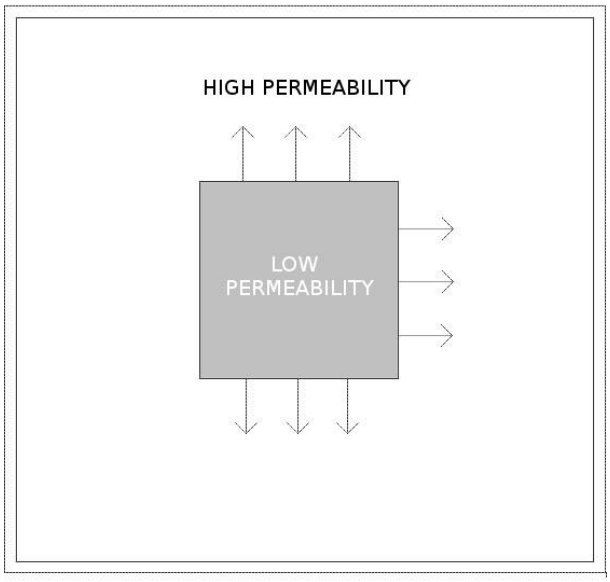

Figure 8 *Low and high permeability regions, geometry 1.*

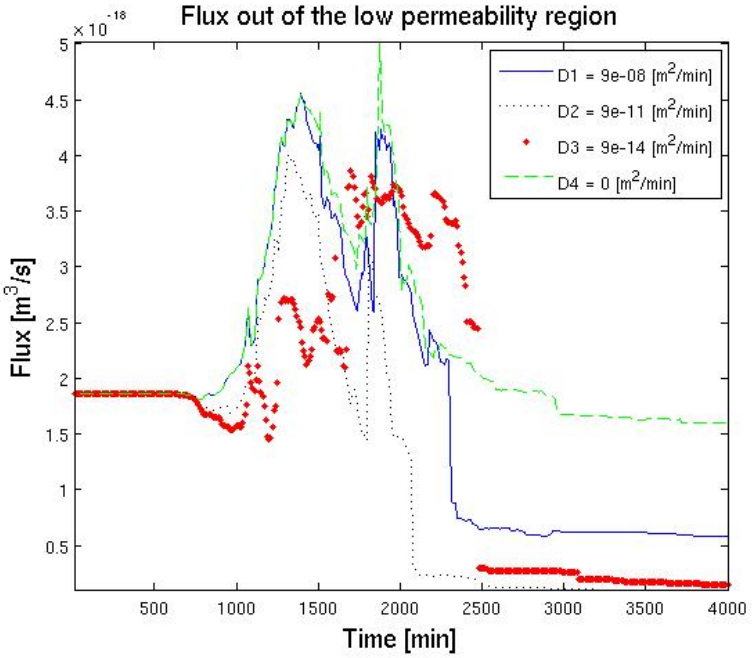

Figure 9 *Flux measure out of the low permeability region, for different values of the diffusion coefficients in water, geometry 1.*

Volume through the low permeability region				
Diffusion Coefficient $[m^2/min]$	Time Interval [min]	Volume $[m^3]$ V_{low}	Volume without biofilm $[m^3]$	Increment $[\%]$
9×10^{-8}	710 - 2480	4.69×10^{-15}	3.29×10^{-15}	27
9×10^{-11}	720 - 1940	3.01×10^{-15}	2.27×10^{-15}	32.5
9×10^{-14}	740 - 2310	4.68×10^{-15}	2.92×10^{-15}	60.2
0	740 - 2920	6.1×10^{-15}	4.06×10^{-15}	50.2

Table 1

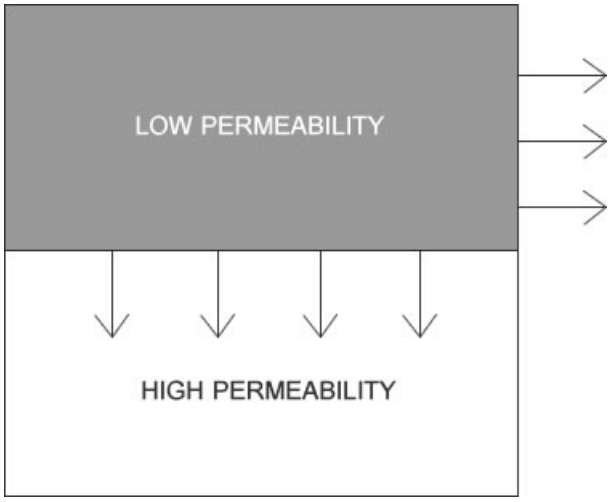

Figure 10 *Low and high permeability regions, geometry 2.*

In order to study the possibility to redirect the flux of water to the low permeability regions, we simulate two areas of different permeability in the network. In both regions, a Rayleigh distribution is assumed for the radius but in the low permeability region, the mean radius is $r_{2_{mean}} = 1.2 \times 10^{-7}[m]$, which is

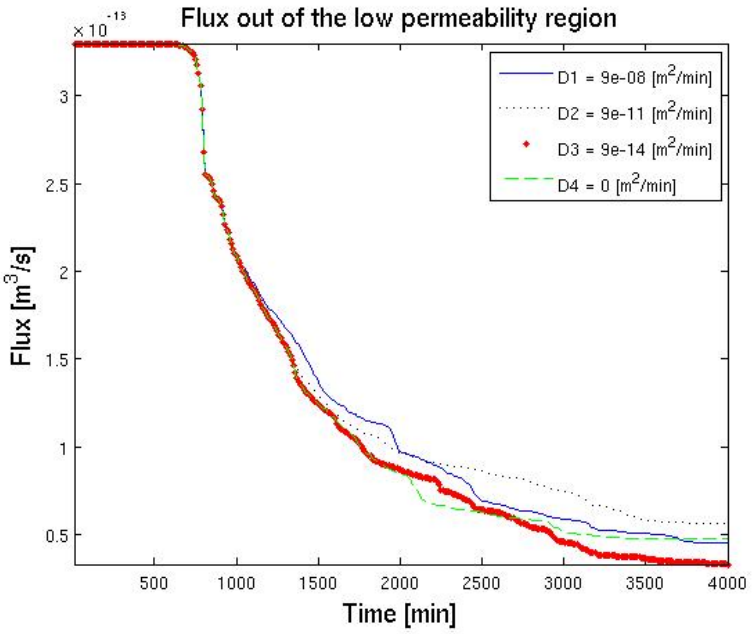

Figure 11 *Flux measure out of the low permeability region, for different values of the diffusion coefficients in water, geometry 2.*

smaller than the mean radius of the high permeability region $r_{1_{mean}} = 12.2 \times 10^{-6}[m]$ (see Table 3). Two sets of simulations with different geometries are performed. The first geometry is shown in Figure 8 and the second geometry is shown in Figure 10. As shown in Figure 8, the low permeability region is placed at the center of the network. In the second geometry, the low permeability region is placed parallel to the high permeability layer.

In Figure 9 the flux out of the low permeability region is shown for the first geometry and for different diffusion coefficients of the nutrients in water. We observe that the flux out of the low permeability region increases for a period between 800 minutes and 2500 minutes approximately. However, to have a better understanding of the effect of selective plugging in flow diverted to low permeability region, the volume of water out of the low permeability region is computed.

The volume out of the low permeability region is computed as follows,

$$V_{low} = \int_{t_0}^{t_f} Q_{low}\, dt. \tag{23}$$

The initial time limit t_0 was set as the time for which the normalized flux started to change and the final time limit t_f was set as the last time for which the flux was above the initial value.

In order to compare the results with the case of the absence of biofilm, the volume out of low permeability region when no biofilm is present is computed within the same time limits.

In Table 1 the results for the volume of water out of the low permeability region for different diffusion coefficients with biofilm growth and without biofilm growth are shown. We observe that the volume of water flowing out of this region increases (compare to the case when no biofilm is present) for all the cases within a period which depends on the diffusion coefficient. We observe an increase between 27 % for a diffusion coefficient of 9×10^{-8} and 60% for a diffusion coefficient of 9×10^{-14} .

We observe that if the diffusion coefficient decreases then the increase in the volume of water is more significant. This is because when the diffusion coefficient decreases the transport of nutrients is dominated by the advection term, then nutrients are mainly located in the high permeability regions, which makes selective plugging more efficient.

Parameters for the simulations without growth of biofilm		
Name	Symbol	Value
Pore length	l	95×10^{-6} $[m]$
Network size in the x direction	L_x	0.019 $[m]$
Network size in the y direction	L_y	0.00095 $[m]$
Number of tubes in the network	N_a	4210
Mean pore radius	r_{mean}	3.5339×10^{-6} $[m]$ [6]
Global pressure gradient (per meter)	ΔP	1.6 $[kPa/m]$
Viscosity of water	μ	$4.7 \times 10^{-}5$ $[Pa \cdot min]$
Density of water	ρ_w	1000 $[kg/m^3]$
Diffusion coefficient of water	D_w	3.9710×10^{-8} $[m^2/min]$ [10]
Inlet reservoir concentration	C_{in}	1 $[kg/m^3]$

Table 2.

In Figure 11 the results for the second geometry are shown. As we can see, for this geometry there is no increase in the flux through the low permeability region. Since the region of low permeability region is half of the network, when the bacteria starts growing in the high permeability region, there is a large tendency to plug the inlet of the high permeability region and hence the flux through the whole network (including the flux through the low permeability region) will decrease faster than in the first case.

Parameters for the simulations with growth of biofilm		
Name	Symbol	Value
Mean pore radius	r_{mean}	12.2×10^{-6} $[m]$ [6]
Mean pore radius 1	$r_{1_{mean}}$	12.2 x $10^{-6}[m]$ [6]
Mean pore radius 2	$r_{2_{mean}}$	1.2 x $10^{-7}[m]$
Pore length	l	95 $\times 10^{-6}$ $[m]$
Global pressure gradient	ΔP	1.6 $[kPa/m]$
Viscosity of water	μ	0.001/60 $[Pa \cdot min]$
Density of water	ρ_w	1000 $[kg/m^3]$
Density of biofilm	ρ_{bf}	20 $[kg/m^3]$ [16]
Yield coefficient	Y	0.34 [2]
Biomass specific growth rate for bacteria	λ_b^+	$60 \times 1.1 \times 10^{-4}$ $[min^{-1}]$ [2]
Biomass specific decay rate for bacteria	λ_b^-	$60 \times 1.1 \times 10^{-6}$ $[min^{-1}]$ [6]
Half saturation constant for bacteria	E_{sb}	2×10^{-3} $[kg/m^3]$ [2]
Biomass specific growth rate for biofilm	λ_{bf}^+	$60 \times 1.1 \times 10^{-4}$ $[min^{-1}]$
Biomass specific decay rate for biofilm	λ_{bf}^-	$60 \times 1.1 \times 10^{-6}$ $[min^{-1}]$
Half saturation constant for biofilm	E_{sbf}	2×10^{-3} $[kg/m^3]$
Inlet reservoir concentration	C_{in}	1 $[kg/m^3]$
Initial biomass concentration	b_0	1×10^{-6} $[kg/m^3]$
Biofilm / bulk water viscosity ratio	β	10^3

Table 3 *T.*

Conclusions

In this work, we studied the biofilm growth in porous media using a two-dimensional pore network model. We assumed that the bacteria, necessary for the biofilm growth, were present in 4% of the tubes. The injection of nutrients for the bacteria population growth was described by an advection diffusion equation. Additionally, in our model we consider that the biofilm is able to spread to the neighboring tubes according to a spreading potential which takes into account the direction of the flux, the velocity and the amount of nutrients available. We studied the hydrodynamic changes caused by biofilm growth using three different geometries for the pore network. In the first geometry, a Raleigh distribution was used for the whole network. In the second geometry, we simulate two areas of different permeability, the area of low permeability was placed in the middle of the network. Finally, we used a layered geometry in which the low permeability region is placed parallel to the high permeability region. For the first case, a decrease in the normalized flux of 90% was observed when 70% of the void space in the network was occupied by biofilm.

In the second case, where two regions of different permeability were simulated, the model shows flow diversion to the low permeability region, and an increase of 60% of the flow volume was observed (compared to the flow out of the low permeability region without biofilm growth). This result might indicate an increase in the sweep efficiency in waterflood techniques, however, a two-phase flow model has to be developed additionally in order to adequately model the production of oil from heterogeneous reservoirs. However, after some time the flux through the low permeability region starts to decrease. Therefore, the injection of nutrients has to be stopped in order to prevent clogging of the low permeability regions. For the third case, the total flux through the low permeability region does not increase, since there is more tendency to plug the inlet in the network. For the second and third geometry diffusion coefficient for water was varied. For the second geometry, it was observed that the flux through the low permeability region was larger when the diffusion coefficient was smaller. It could be of greatest interest to investigate the dependence of the sweep efficiency on other parameters such as the pressure drop in the network, the coefficient of bacterial growth or the concentration of nutrients in the network. Finally, the results obtained in this work can be used for a future up-scaling technique to the real reservoir scale in oil reservoir simulations.

Acknowledgements

We thank the Mexican Institute of Petroleum (IMP) for financially supporting this research through the 'Programa de Captación de Talento, Reclutamiento, Evaluación y Selección de Recursos Humanos (PCTRES)' grant.

References

[1] Armstrong, R. and Wildenschild, D. [2012] Investigating the pore-scale mechanisms of microbial enhanced oil recovery. *Journal of Petroleum Science and Engineering*, **94-95**, 155–164.

[2] Bakke, R., Trulear, M., Robinson, J. and Characklis, W. [1984] Activity of Pseudomonas aeruginosa in biofilms: steady state. *Biotechnology and bioengineering*, **26**(12), 1418–1424.

[3] Behlulgil, K., Mehmetoglu, T. and Donmez, S. [1992] Application of microbial enhanced oil recovery technique to a Turkish heavy oil. *Applied microbiology and biotechnology*, **36**(6), 833–835.

[4] Bryant, S.L., Lockhart, T.P. et al. [2000] Reservoir engineering analysis of microbial enhanced oil recovery. In: *SPE Annual Technical Conference and Exhibition*. Society of Petroleum Engineers.

[5] Chen-Charpentier, B. [1999] Numerical simulation of biofilm growth in porous media. *Journal of computational and applied mathematics.*, **103**, 55–66.

[6] Ezeuko, C., Sen, A., A., G. and Gates, I. [2011] Pore-network modelling of biofilm evolution in porous media. *Biotechnology and Bioengineering*, **108**(10), 2413–2423.

[7] Ezeuko, C., Sen, A. and Gates, I. [2013] Modelling biofilm-induced formation damage and biocide treatment in subsurface geosystems. *Microbial biotechnology*, **6**(1), 53–66.

[8] Jack, T., Stehmeier, L., Islam, M. and Ferris, F. [1991] Ch. F-6 Microbial Selective Plugging to Control Water Channeling. *Developments in Petroleum Science*, **31**, 433–440.

[9] Kim, D.S. and Fogler, H.S. [2000] Biomass evolution in porous media and its effects on permeability under starvation conditions. *Biotechnology and bioengineering*, **69**, 47–56.
[10] Lawrence, J., Wolfaardt, G. and Korber, D. [1994] Determination of diffusion coefficients in biofilms by confocal laser microscopy. *Applied and environmental microbiology*, **60**(4), 1166–1173.
[11] Li, Q., Kang, C., Wang, H., Liu, C. and Zhang, C. [2002] Application of microbial enhanced oil recovery technique to Daqing Oilfield. *Biochemical Engineering Journal*, **11**(2), 197–199.
[12] Picioreanu, C., Kreft, J.U. and van Loosdrecht, M.C. [2004] Particle-based multidimensional multispecies biofilm model. *Applied and environmental microbiology*, **70**(5), 3024–3040.
[13] Pintelon, T., Graf von der Schulenburg, D. and Johns, M. [2009] Towards optimum permeability reduction in porous media using biofilm growth simulations. *Biotechnology and Bioengineering*, **103**(4), 767–779.
[14] Raiders, R.A., Knapp, R.M. and McInerney, M.J. [1989] Microbial selective plugging and enhanced oil recovery. *Journal of industrial microbiology*, **4**(3), 215–229.
[15] Raoof, A. and Hassanizadeh, S.M. [2010] A new method for generating pore-network models of porous media. *Transport in porous media*, **81**(3), 391–407.
[16] Ro, K.S. and Neethling, J. [1991] Biofilm density for biological fluidized beds. *Research journal of the water pollution control federation*, 815–818.
[17] Graf von der Schulenburg, D., Pintelon, T., Picioreanu, C., van Loosdrecht, M. and Johns, M. [2008] Three-dimensional simulations of biofilm growth in porous media. *AIChe Journal*, **55**(2), 494–504.
[18] Sen, R. [2008] Biotechnology in petroleum recovery: the microbial EOR. *Progress in Energy and Combustion Science*, **34**(6), 714–724.
[19] Sheehy, A. et al. [1990] Field studies of microbial EOR. In: *SPE/DOE Enhanced Oil Recovery Symposium*. Society of Petroleum Engineers.
[20] Suchomel, B., Chen, B. and Allen, M. [1998] Macroscale properties of porous media from a network model of biofilm processes. *Transport in porous media.*, **31**, 39–66.
[21] Thullner, M. and Baveye, P. [2008] Computational pore network modeling of the influence of biofilm permeability on bioclogging in porous media. *Biotechnology and Bioengineering*, **99**(6), 1337–1351.
[22] Thullner, M., Zeyer, J. and Kinzelbach, W. [2002] Influence of microbial growth on hydraulic properties of pore networks. *Transport in porous media.*, **49**, 99–122.
[23] Van Wijngaarden, W., Vermolen, F., Van Meurs, G. and Vuik, C. [2012] A mathematical model and analytical solution for the fixation of bacteria in Biogrout. *Transport in porous media*, **92**(3), 847–866.
[24] Warrick, A.W. [2003] *Soil water dynamics*. Oxford University Press, USA.
[25] Yakimov, M.M., Amro, M.M., Bock, M., Boseker, K., Fredrickson, H.L., Kessel, D.G. and Timmis, K.N. [1997] The potential of Bacillus licheniformis strains for in situ enhanced oil recovery. *Journal of Petroleum Science and Engineering*, **18**(1), 147–160.